

Wavelet-based cross-correlation analysis of the scaling in molecular clouds

Tigran Arshakian & Volker Ossenkopf

Overview

We develop a wavelet-based cross-correlation (WCC) method to study the correlation between structural changes in molecular clouds as a function of scale. The method compares a pair of maps observed in different tracers or at different velocity ranges.

Advantages of the WCC method:

- Allows to measure the correlation coefficient and structural offset between two maps as a function of scale.
- Allows to weight individual pixels by their observational significance.
- Is robust against the noise.

Application of the WCC to simulated fBm (fractional Brownian motion) maps reveals that:

- Cross-correlation coefficient can strongly depend on the scale.
- Correlation coefficient and offset can be recovered robustly regardless of noise.

Analysis of the G333 molecular line maps (^{13}CO and C^{18}O) shows:

- A large scale gradient in the structural distribution. This could indicate a density structure where every core shows a low density tail towards the South-West mainly seen in ^{13}CO .

The WCC can be used to trace the correlated structural changes between different maps of a molecular cloud at scales representing the structural and physical importance such as chemical and phase transitions.

Wavelet cross-correlation (WCC)

Wavelet transform is proven to be a powerful tool for the scaling analysis in galaxies, interstellar clouds (Stutzki et al. 1998; Frick et al. 2001; Ossenkopf et al. 2008, hereafter O08). Convolution of the wavelet filter $\psi(l, \mathbf{r})$ ($\mathbf{r} = (x, y)$) with an image $f(\mathbf{r})$ filters the image on a scale l given by the wavelet:

$$F(\mathbf{r}, l) = \iint f(\mathbf{r}') \psi(l, \mathbf{r} - \mathbf{r}') d\mathbf{r}'$$

Optimal wavelet filter for molecular clouds is found to be the Mexican-hat filter (O08), which provides the correct power spectral slope and spectral features:

$$\psi(\mathbf{r}) = \psi_c(\mathbf{r}) + \psi_a(\mathbf{r}) = \frac{4}{\pi^2} \exp\left(-\frac{r^2}{(l/2)^2}\right) + \frac{4}{\pi^2} \exp\left(-\frac{r^2}{(v l/2)^2}\right) - \exp\left(-\frac{r^2}{(l/2)^2}\right),$$

where $\psi_c(\mathbf{r})$ and $\psi_a(\mathbf{r})$ are the core and annulus of the filter, and $v = 1.5$ is the diameter ratio between the annulus and the core.

The Δ -variance (O08) of the filtered map $F(\mathbf{r}, l)$ and its weights $w_F(\mathbf{r}, l)$, indicating the significance of each pixel of the image, shows characteristic scales and the power spectral slope in the individual maps.

To study the cross-correlation of the amount of structure between two maps, f and g , on different scales, we introduce the **wavelet-based cross-power spectrum**,

$$C_l(\boldsymbol{\tau}) = \frac{C(l, \boldsymbol{\tau})}{\sigma_F(l) \sigma_G(l)} \quad (1)$$

where

$$C(l, \boldsymbol{\tau}) = \iint_{x,y} \sqrt{w_F(\mathbf{r}, l) w_G(\mathbf{r} + \boldsymbol{\tau}, l)} F_w^*(\mathbf{r}, l) G_w(\mathbf{r} + \boldsymbol{\tau}, l) d\mathbf{r}.$$

$$\sigma_F(l) = \left(\iint_{x,y} w_F(\mathbf{r}, l) F_w^2(\mathbf{r}, l) d\mathbf{r} \right)^{1/2}, \quad \sigma_G(l) = \left(\iint_{x,y} w_G(\mathbf{r}, l) G_w^2(\mathbf{r}, l) d\mathbf{r} \right)^{1/2}$$

and

$$F_w = F(\mathbf{r}, l) - \bar{F}_w(l), \quad G_w = G(\mathbf{r}, l) - \bar{G}_w(l),$$

where

$$\bar{F}_w(l) = \frac{\iint w_F(\mathbf{r}, l) F(\mathbf{r}, l) d\mathbf{r}}{\iint w_F(\mathbf{r}, l) d\mathbf{r}}, \quad \bar{G}_w(l) = \frac{\iint w_G(\mathbf{r}, l) G(\mathbf{r}, l) d\mathbf{r}}{\iint w_G(\mathbf{r}, l) d\mathbf{r}}$$

are weighted means of two maps respectively.

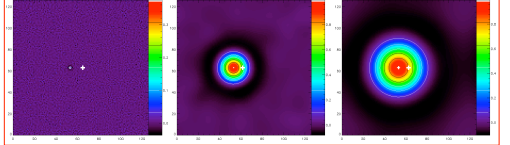
Cross-power spectrum (Eq. (1); see Fig 1) is used to estimate the **correlation coefficient $r(l)$** on scale l ,

$$r(l) = C_l(\boldsymbol{\tau} = \mathbf{0}) \quad (2)$$

and **offset vector $\boldsymbol{\tau}(l) = [\Delta x, \Delta y]$** , where the Δx and Δy give the location of the correlation peak of cross-power spectrum

$$\boldsymbol{\tau}_{\max}([\Delta x, \Delta y], l) = \arg \max_{x,y} C_l(\boldsymbol{\tau}).$$

Figure 1. Cross-power spectrum of two fBm maps (see, for example, Fig. 3, top panel) for scales of 1 pix, 15 pix, and 30 pix. Offset between fBm maps is 10 pix along the X-axis. The distance between the peak of the maximum correlation and the map center (white cross) shows the offset $\boldsymbol{\tau}(l) = 10$ pix between maps and the center of the cross-power spectrum gives the correlation coefficient $r(l)$ (see Eq. (2)).



Simple tests

We start testing the WCC for two simulated circular structures having Gaussian intensity profiles with amplitude=1 and standard deviations of 3 pix and 5 pix, which are offset by 5 pix along Y-axis (Fig. 2, top panel). The size of the Gaussians is traced by the maxima in the Δ -variance spectra (10-15 pix; 2nd panel). Correlation coefficient strongly depends on scale becoming large above the dominant structure scales. Amplitude and direction of the offset $\boldsymbol{\tau}(l)$ (bottom panel) are correctly recovered on those scales.

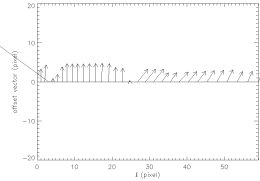
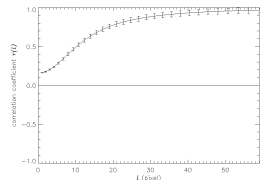
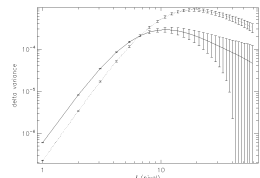
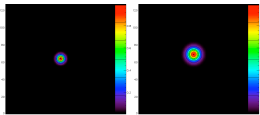


Figure 2. Top panels. Maps of Gaussian intensity profile. 2nd panel. Δ -variance of two maps (full and dotted lines represent the 1st and 2nd map, respectively). 3rd panel. WCC function (full line) dependence of cross-correlation coefficient on scale. Bottom panel. Offset vector as a function of scale: the vector shows the offset with respect to the first image.

We also compared two fBm maps with spectral index of 3 (Fig. 3, top panel) where the second map is the filtered (maximum filter with a size of 15 pix) version of the first map, which mimics the opacity of optically thick lines. Correlation is negligible at small scales and it becomes significant at $l \geq 30$ pix (3rd panel). The correlation coefficient turns negative at scales below the mutual offset. The offset vector (length and direction) is exactly recovered for $l \geq 8$ pix (bottom panel).

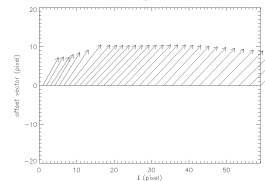
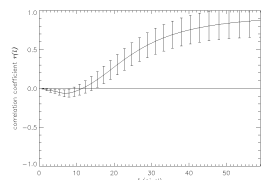
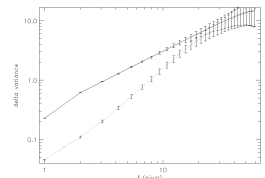
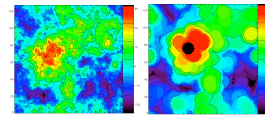


Figure 3. Analysis for original fBm map (left) and the same map filtered on scale of 15 pix and shifted for 14 pix in Nord-West direction (10 pix along X-axis and 10 pix along Y-axis). Description of panels as in Fig. 2.

Realistic tests

In reality the offset can vary on different spatial scales. To test this, we generate a fBm map with $S/N=10$ (Fig. 4, top left panel) and use the Fourier shift theorem to shift the large scales ($l \geq 10$ pix) by 18 pix in the South-West direction (top right panel). The Δ -variance spectrum has a bump at small scales due to low S/N value (2nd panel). Application of the WCC for these two maps shows that the offset vector can be recovered robustly (bottom panel). Structures are correlated significantly at small scales ($l < 10$ pix) as expected from the construction of the maps. The correlation gradually decreases from 10 to 20 pix (3rd panel) due to the shift of a structure at scales $l > 10$ pix. At scales of ≥ 20 pixels the structure sizes exceed the offset so that we find a gradual increase of the correlation coefficient at large scales.

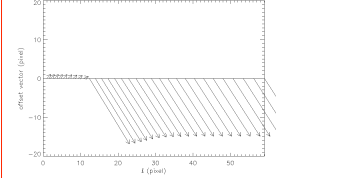
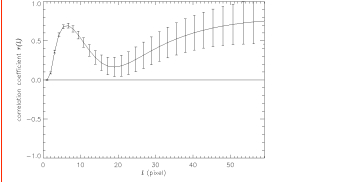
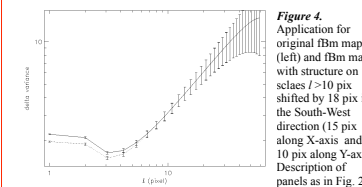
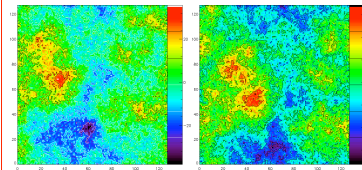


Figure 4. Application for original fBm map (left) and fBm map with structure on scales $l > 10$ pix shifted by 18 pix in the South-West direction (15 pix along X-axis and 10 pix along Y-axis). Description of panels as in Fig. 2.

Application to GMC G333

We applied the WCC to the maps of the giant molecular cloud (GMC) G333 observed in ^{13}CO and C^{18}O (Lo et al. 2009; Fig. 5, top panels). Their Δ -variance spectra have pronounced structure on scales of about 30 pix and 50 pix respectively and the structure is strongly correlated at scales > 5 pix (3rd panel). Large differences between the maps only occur at small scales affected by noise. The structure is offset at scales larger than 40 pix with amplitude of ~ 5 pix along the filament, where all structures in ^{13}CO are shifted to the South-West relative to C^{18}O . This could indicate a large-scale column density gradient enhancing the structure in ^{13}CO in that direction.

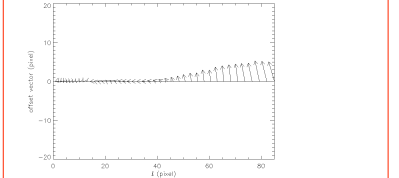
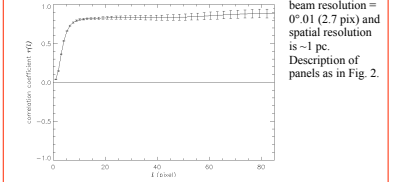
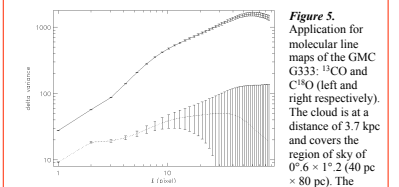
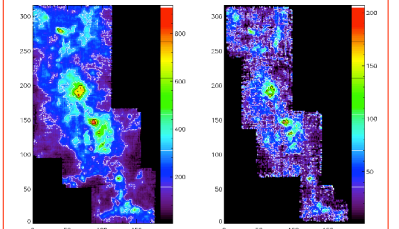


Figure 5. Application for molecular line maps of the GMC G333: ^{13}CO and C^{18}O (left and right respectively). The cloud is at a distance of 3.7 kpc and covers the region of sky of $0^\circ 6' \times 1^\circ 2'$ (40 pc \times 80 pc). The beam resolution = $0''.01$ (2.7 pix) and spatial resolution is ~ 1 pc. Description of panels as in Fig. 2.